Separation Science and Technology
Publication details, including instructions for authors and subscription information:
http://www.informaworld.com/smpp/title~content=t713708471

A Study of Retention in Thermal Field-Flow Fractionation

Marcus N. Myers[a]; Karin D. Caldwell[a]; J. Calvin Giddings[a]
[a] DEPARTMENT OF CHEMISTRY, UNIVERSITY OF UTAH, SALT LAKE CITY, UTAH

To cite this Article Myers, Marcus N. , Caldwell, Karin D. and Giddings, J. Calvin(1974) 'A Study of Retention in Thermal Field-Flow Fractionation', Separation Science and Technology, 9: 1, 47 — 70

To link to this Article: DOI: 10.1080/01496397408080043

URL: http://dx.doi.org/10.1080/01496397408080043

SEPARATION SCIENCE, 9(1), pp. 47–70, 1974

A Study of Retention in Thermal Field-Flow Fractionation

MARCUS N. MYERS, KARIN D. CALDWELL, and
J. CALVIN GIDDINGS

DEPARTMENT OF CHEMISTRY
UNIVERSITY OF UTAH
SALT LAKE CITY, UTAH 84112

Abstract

A broad theoretical and experimental investigation of retention in thermal field-flow fractionation is reported here. Equations connecting retention parameters with underlying thermal diffusion constants are reviewed, and new equations are developed to account for the distortion of the flow profile caused by a variable viscosity. Parameters investigated experimentally include channel width, solute molecular weight, channel temperature drop, cold-wall temperature, sample size, and solvent effects. All but the last two of these experimental studies showed good conformity with theoretical predictions. No theory exists for the prediction of sample-size or solvent effects. With regard to the latter, experimental results show that a variety of organic solvents are very effective, at roughly equal levels, in providing retention, while aqueous solvents are generally ineffective.

INTRODUCTION

Thermal field-flow fractionation (TFFF) is a method in which a temperature difference, superimposed across the parabolic or near-parabolic velocity profile of a fluid flowing between parallel plates, is used for separating macromolecules. The method has been tested successfully using polystyrene solutes of different molecular weights in toluene (*1*).

Despite the fact that some major theoretical and experimental aspects of column performance have been investigated for TFFF (*2*), virtually none of the factors controlling retention have been systematically studied. Separation in TFFF, as in chromatography, is achieved by differential retention, so that it is imperative to characterize retention factors as a prelude to the task of designing effective TFFF systems. One might expect some help in this task from the literature on thermal diffusion, since the thermal diffusion phenomenon is the root-cause of retention. However, the aid from this source is minimal. No satisfactory theory for thermal diffusion in the liquid state has evolved (*3*). Experimental work with polymers is extremely limited, and tends to exhibit inconsistencies (*4*). We are left with only a few useful generalizations from the literature—generalizations, for instance, that state that most solutes diffuse toward the cold wall (*3*), or that the coefficient of thermal diffusion, D', tends to remain constant with changes in the molecular weight of polymer solutes (*5*, *6*).

The paucity of reliable data from conventional studies of thermal diffusion has led us to suggest that TFFF might be an effective tool for measuring thermal diffusion parameters (*4*). Indeed, the data collected in these studies have confirmed the value of TFFF in this role. These results will be reported subsequently (*7*).

The following expression describes the molar thermal and diffusive fluxes of a particular chemical species exposed to temperature and concentration gradients along axis x (*8*, *2*):

$$J = -D\left[\frac{dc}{dx} + c\gamma\,\frac{dT}{dx}\right] - D'c\,\frac{dT}{dx} \tag{1}$$

Here D is the diffusion coefficient, c is molar concentration, γ is the coefficient of thermal expansion, and D' is the coefficient of thermal diffusion. Introduction of the thermal diffusion factor, $\alpha = D'T/D$, transforms the above expression into

$$J = -D\left[\frac{dc}{dx} + \left(\frac{\alpha}{T} + \gamma\right)c\,\frac{dT}{dx}\right] \tag{2}$$

Under steady-state conditions in which the flux, J, is zero, Eq. (2) reduces to the simple differential equation

$$\frac{d\ln c}{dx} = -\left(\frac{\alpha}{T} + \gamma\right)\frac{dT}{dx} = -\frac{1}{\ell} \tag{3}$$

The solution to this equation provides the steady-state concentration distribution in the x-direction. When ℓ is assumed constant, the solution acquires a simple exponential form

$$c^* = c_0 \exp(-x/\ell) \tag{4}$$

where c^* denotes a steady-state concentration.

Parameter ℓ is the mean height of the exponential solute cloud. This parameter is of paramount importance in characterizing any field-flow fractionation system (*9*, *10*). All the variations in retention observed in this study ultimately reflect variation in parameter ℓ. This parameter, in turn, hinges on thermal diffusion factor α and on thermal diffusion coefficient D' in accordance with the above equations.

THEORY OF RETENTION

Retention in field-flow fractionation is characterized by the retention parameter, R (= zone velocity/average fluid velocity). Parabolic flow of a uniform fluid between two flat plates, parallel in orientation, and a distance w apart, leads to the following expression for R (*2*):

$$R = 6\lambda[\coth(1/2\lambda) - 2\lambda] \tag{5}$$

where λ is the dimensionless parameter, ℓ/w. This expression provides an excellent approximation for most forms of field-flow fractionation, but is less accurate for TFFF, for reasons elaborated below.

Retention in TFFF is complicated by the distortion of the flow profile resulting from the variable viscosity—a variability induced by the temperature gradient. This effect was illustrated earlier by some computer calculations (*2*), showing that the error of the isoviscous model, Eq. (5), was of the order of 10%. (Unfortunately, the labels for the top and bottom curves of Fig. 1 in Ref. 2 were transposed—suggesting an effect opposite in direction to that actually calculated.) We now present the theoretical basis needed for retention calculations in TFFF.

The velocity profile for laminar flow occurring in a channel consisting of the flow space between two parallel plates is determined by the equation (*11*)

$$\frac{d^2v}{dx^2} = -\Delta P/L\eta \tag{6}$$

where v is the fluid velocity, x is the distance from the bottom surface of the channel, ΔP is the pressure drop used to make flow occur over distance L, and η is the fluid viscosity. When a temperature difference exists between the top and bottom plates, η varies with altitude x. Integration of Eq. (6) under this condition yields the general expression

$$v = \frac{-\Delta P}{L} \iint \frac{(dx)^2}{\eta} + k_1 x + k_2 \tag{7}$$

where integration constants k_1 and k_2 are fixed by the condition that v must vanish at the two walls, $x = 0$ and $x = w$.

The exact form of the dependence of viscosity, η, upon distance x is not known. In order to achieve an integrable form for Eq. (7), we make the following assumptions. First, we assume for convenience that the thermal conductivity is constant over the working temperature range of TFFF. (The variation, in fact, is sometimes as high as 10%—not entirely negligible. We shall return later to this topic.) This assumption leads to a linear temperature profile. Second, while no exact formula is known for the dependence of viscosity on temperature, the exponential expression

$$\eta = \eta_0 \exp(B/T) \tag{8}$$

is commonly assumed and is moderately consistent with both experimental data and approximate liquid theories. This expression, when used in Eq. (7), requires numerical integration. Since it is not exact anyway, we seek a modification that is integrable in closed form.

If T is written as $T_c + \tau$, then Eq. (8) takes the form

$$\eta = \eta_0 \exp\left[\frac{B}{T_c}\frac{1}{(1 + \tau/T_c)}\right] \tag{9}$$

The quantity $1/(1 + \tau/T_c)$ can then be expanded in the following series:

$$1/(1 + \tau/T_c) = 1 - (\tau/T_c) + (\tau/T_c)^2 - \cdots \tag{10}$$

If the temperature increment, τ, above the cold-wall temperature, T_c, is small compared to T_c itself, a good approximation results if only two terms are retained. Equation (9) then becomes

$$\eta = \eta_0 \exp(B/T_c) \exp(-B\tau/T_c^2) = \eta_c \exp(-B\tau/T_c^2) \tag{11}$$

where η_c is the viscosity at the cold wall. If τ is replaced by $x\Delta T/w$—where ΔT is the total temperature drop across the channel width w—then η acquires the necessary distance (x)-dependent form

$$\eta = \eta_c \exp(-\beta x/w) \tag{12}$$

where $\beta = B\Delta T/T_c^2$. The variation of η by this approximation is compared to its variation according to Eq. (8) or (9) in Fig. 1. Although the assumed ΔT is a rather large 100°C, the curves diverge significantly only near the hot wall, $(x/w) = 1$.

The substitution of Eq. (12) into Eq. (7) provides an integrable form which, together with the stated boundary conditions, yields the velocity profile

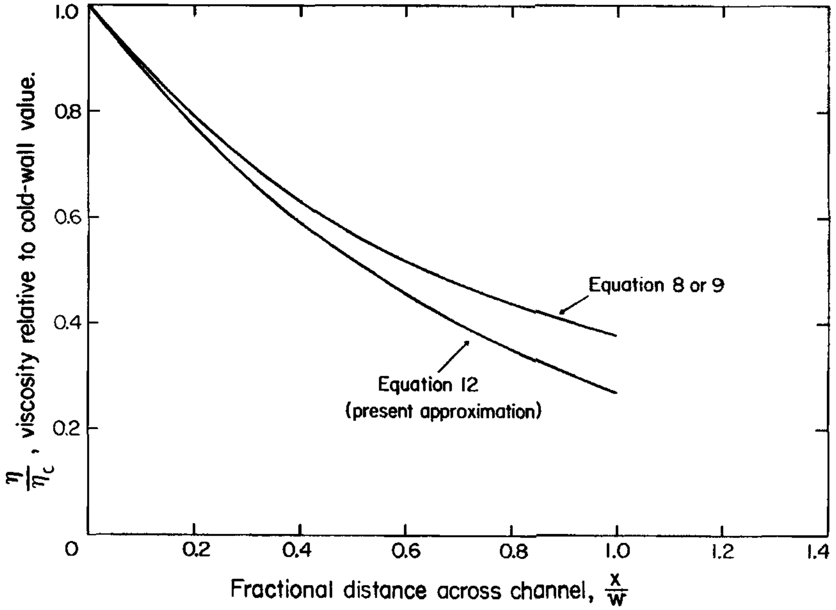

FIG. 1. The variation of viscosity across a channel of ethylbenzene solvent ($B = 1095$°C) with $T_c = 16$°C and $\Delta T = 100$°C. The approximation of Eq. (12), lower curve, is excellent except near the hot wall at $(x/w) = 1$.

$$v = \frac{-\Delta P}{L\eta_c}\frac{w^2}{\beta^2}\left[\exp\left(\frac{\beta x}{w}\right) - 1 + \frac{x}{w}(1 - \exp \beta)\right] \tag{13}$$

This velocity profile is slightly asymmetric, having a peak flow velocity at the point

$$\left(\frac{x}{w}\right)_{\max} = \frac{1}{\beta}\ln\left(\frac{\exp \beta - 1}{\beta}\right) \tag{14}$$

The asymmetry is illustrated in Fig. 2.

The average fluid velocity in the channel is calculated from the above as

$$\langle v\rangle = \frac{\int_0^w v\,dx}{w} = \frac{-\Delta P}{L\eta_c}\frac{w^2}{\beta^2}\left[(\exp \beta - 1)\left(\frac{1}{\beta} - \frac{1}{2}\right) - 1\right] \tag{15}$$

With this, retention parameter R can be obtained by the equation (*2*)

$$R = \langle c^* v\rangle / \langle c^*\rangle\langle v\rangle \tag{16}$$

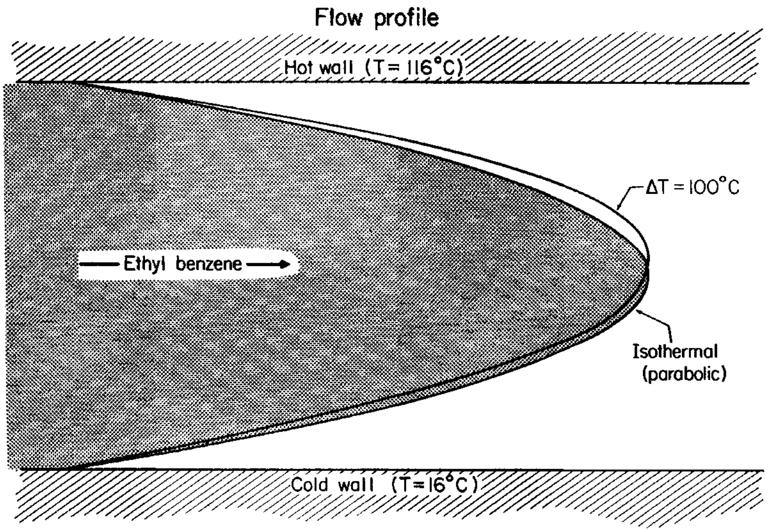

FIG. 2. Asymmetry of the flow profile for ethylbenzene at $T_c = 16\,^\circ\mathrm{C}$ and $\Delta T = 100\,^\circ\mathrm{C}$ ($\beta = 1.31$). Peak flow occurs at $(x/w) = 0.554$. The symmetrical, parabolic profile with the same average velocity is shown for comparison.

This expression, in conjuction with Eqs. (4), (13), and (15), yields the key retention formula

$$R = \frac{\dfrac{2\lambda\beta}{1 - \beta\lambda}[(\beta\lambda + \beta - 1)\exp(\beta - 1/\lambda) + \beta\lambda - \beta - 1] + 2\lambda\beta[\exp(-1/\lambda) + \exp\beta]}{[1 - \exp(-1/\lambda)][(\beta - 2)\exp\beta + \beta + 2]} \qquad (17)$$

Figure 3 shows the dependence of R on λ predicted by Eq. (17) for various values of the parameter $\beta = B\Delta T/T_c^2$. The curve for $\beta = 0$ is also obtainable from Eq. (5). From these curves it is clear that the distortion of the velocity profile by the variable viscosity does not have a profound effect on retention under ordinary experimental conditions. However, the departure from the isoviscous curve, $\beta = 0$, is measurable, and the necessary correction should be applied in careful work.

Figure 4 makes these points more specific. This graph shows the influence of parameter B on retention for various λ values under specific (but typical) temperature conditons. The range of B is considerably extended in this plot to show the extreme effects of viscosity variations. For most solvents, B is near 1000°K, but for a few it goes considerably higher (e.g., $B = 5150\,^\circ\mathrm{K}$ for formamide).

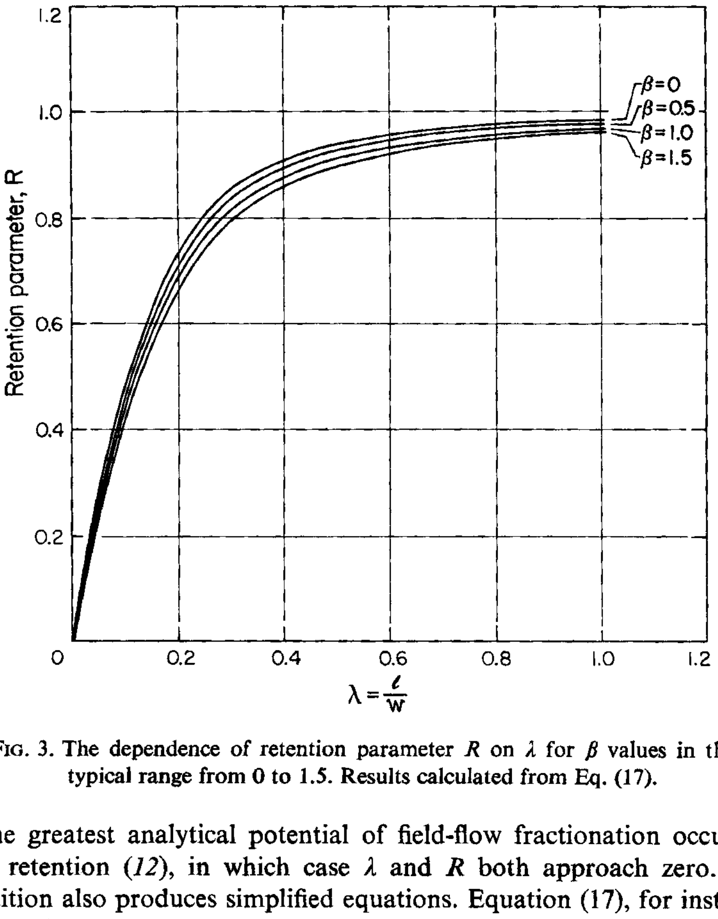

FIG. 3. The dependence of retention parameter R on λ for β values in the typical range from 0 to 1.5. Results calculated from Eq. (17).

The greatest analytical potential of field-flow fractionation occurs at high retention (*12*), in which case λ and R both approach zero. This condition also produces simplified equations. Equation (17), for instance, goes to the limiting form

$$R = \frac{2\lambda\beta(\exp \beta - \beta - 1)}{(\beta - 2)\exp \beta + \beta + 2} \tag{18}$$

as λ approaches zero. If exp β is expanded and terms of high order are neglected, the result is

$$R = 6\lambda(1 - \beta/6) \tag{19}$$

This is an excellent approximation to Eq. (18) even for β values as large as unity (2% error in R). It shows in simple fashion how the existence of variable viscosity, reflected in β, alters the normal limiting expression, $R = 6\lambda$, obtainable from Eq. (5).

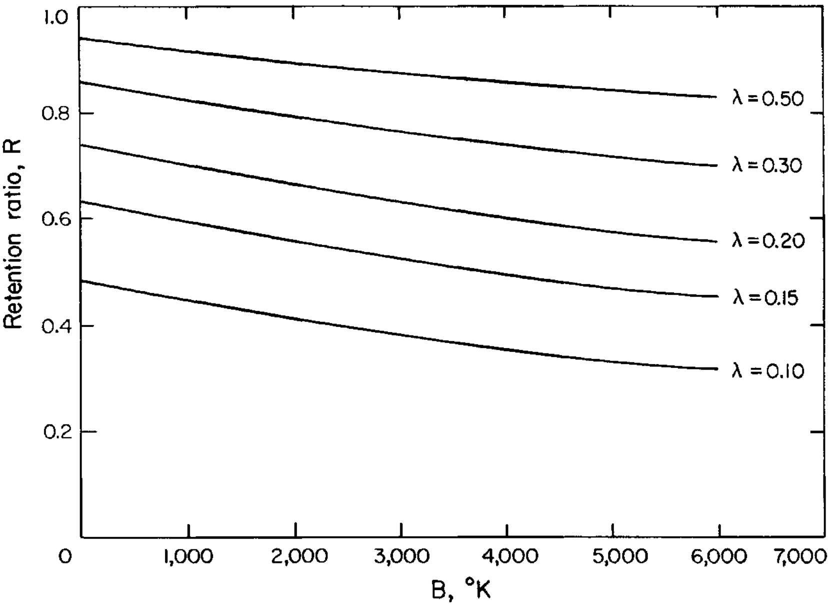

FIG. 4. The variation of R with B at a cold-wall temperature, T_c, of 16°C and at $\Delta T = 60$°C.

The validity of the approximate approach used to obtain Eq. (17) requires further scrutiny. It is necessary, first, to ascertain whether the substitution of Eq. (11) for Eq. (8) in integral expression (7) causes significant error. In order to determine this, Eq. (8) was expanded in a power series, substituted into Eq. (7), and integrated term by term. This convergent series was summed by computer, using sufficient terms to give five significant figures. The R vs λ curves calculated in this way were nearly identical with those obtained from Eq. (16) and shown in Fig. 3. The slight difference in these results is illustrated in Fig. 5. For the most part the two approaches generate a divergence that remains considerably under 0.01 R units.

A second question revolves around the error incurred in assuming a linear temperature profile when, in fact, the thermal conductivity may vary by amounts up to 10% across the channel. This variation will cause an additional distortion in the flow profile. We note, however, that the major profile distortion examined above—resulting from viscosity variations over a linear temperature profile—does not greatly alter the R vs λ curves of Fig. 3. The additional distortion caused by nonconstant thermal con-

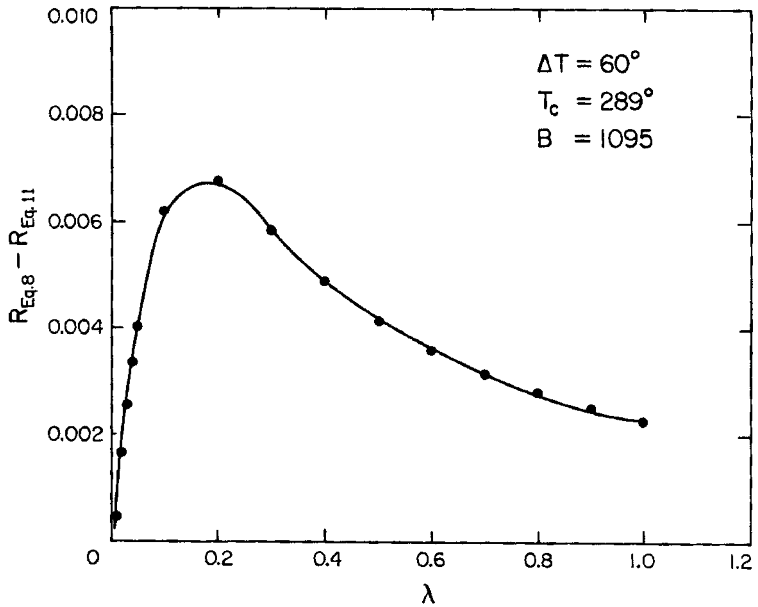

FIG. 5. Divergence of theoretical R values, representing the difference in results between taking Eq. (8) and Eq. (11) for the fundamental temperature dependence of viscosity. This particular curve applies to ethylbenzene solvent with $T_c = 16°C$ and $\Delta T = 60°C$.

ductivity is expected to have only a second-order effect on the R vs λ curves.

The variable thermal conductivity has another effect, however. The temperature gradient, dT/dx, will vary across the channel in inverse proportion to thermal conductivity. The value of dT/dx required for use in Eq. (3) must therefore be selected carefully. The function of Eq. (3) is to provide the link between the thermal diffusion factor, α, and the TFFF parameter, ℓ (or λ). Since α is not well understood, the purposes of this paper can be served by ignoring the rather small variations in dT/dx. The detailed effect of the variability of dT/dx on measuring α values using TFFF will be discussed in another place (*7*).

EXPERIMENTAL

The principal TFFF column used in this work consisted of two copper bars with highly polished faces clamped together over a 0.01-in. (0.254-mm)

Mylar spacer. A flow channel of the desired dimensions was cut out of the spacer. The channel dimensions were 2.54 cm in breadth by 35.6 cm long, with tapered ends. The hot bar was heated by two 500-W electrical cartridge heaters controlled by variable transformers. The cold bar had three holes drilled the entire length, allowing coolant to enter by the center hole and exit by the two outer holes. Both the top and bottom bars had small holes drilled to within 0.76 mm of the surface for temperature measurement by either iron-constantan thermocouples or Yellow Springs Instruments No. 44201 thermistors. Measurements across the breadth of the channel showed a variation of less than 1° Celsius. The temperature measurements along the length of the channel indicated a maximum variation of 1.5°C.

Two 1-mm holes at the apex of the channel's taper formed the inlet and exit for the column. Samples were injected into the flowing solvent at the inlet of the column with a 10-μl syringe. Most of the data was obtained with ultranarrow polystyrene fractions ($M_w/M_n < 1.009$) supplied by Waters Associates. Some of the data for the solvent effects and sample size studies also used polystyrene fractions ($M_w/M_n = 1.06$) supplied by Pressure Chemical Co.

Several "stop-flow" experiments were done to check the results of the continuous-flow data. With the stop-flow method, injection was made under static conditions. Flow was commenced approximately 10 min later, well after the steady-state concentration was established.

A Chromatronix CMP IV pump supplied carrier flow. Mean fluid velocities in the column, $\langle v \rangle$, were generally in the range 0.023 to 0.026 cm/sec for the wide channel and roughly half of this for the narrow channel. Peak detection was obtained with a Waters Associates R401 Refractive Index Monitor. The retention ratio, R, was measured by comparing the polystyrene elution time or volume to that of the void peak obtained from the toluene or dioxane present in (or deliberately introduced into) the polystyrene samples. Reagent grade solvents were used in all studies.

The study of channel-width effects was carried out by using another spacer, having 0.005 in. (0.127 mm) of thickness, between the same copper bars. The other channel dimensions remained identical.

Three other TFFF columns, virtually identical to the one described at the beginning of this section, were used at various times to check the validity of the results from the primary experimental system.

The studies using aqueous solutions were conducted in a system in which a 0.25-mm (nominal) layer of gold was bonded to the copper bats. The channel, now between two gold surfaces, was fixed in dimensions by a 0.254-mm Mylar spacer with a cutout 86.5 cm long by 1.72 cm in breadth. A 1500-W strip heater was clamped to the top bar for heating, while the bottom bar was cooled through direct exposure to coolant. Temperature measurements were made in narrow holes extending entirely through the copper bar and terminating at the gold surface.

Four or five repetitious runs were made and averaged to establish most of the experimental points reported in this work.

RESULTS AND CONCLUSIONS

Repetitious runs under identical conditions generally yielded results with a range of 0.01 to 0.02 *R* units. The typical averaging of four of five such runs should therefore provide results reproducible to something less than 0.01 *R* units.

The alternate columns, used to check the results of the principal column of this work, produced results in close accord under several experimental conditions. The divergence was ordinarily about 0.01 *R* units, with no trend apparent. In view of the above, this divergence cannot be ascribed statistical significance.

It was noted in an earlier paper that peak retention can be affected by the relaxation phenomenon (*2*). Relaxation is the processes in which solute entering the temperature gradient of the column alters its concentration from uniform to exponential. The *R* value is momentarily unity at the beginning of this process, but rather quickly relaxes to the steady-state value under discussion. The short duration in which *R* is abnormally high shifts the measured *R* values to levels slightly above the true steady-state values. The degree of this shift depends on flow velocity, channel width, molecular weight, temperature, and temperature drop. It becomes negligible at extremely low flow rates. However, experimental operation at very low flow velocities is unduly time consuming. The velocity range noted earlier, 0.023 to 0.026 cm/sec, is a compromise level, slow enough to ensure us that relaxation effects are not of major importance, but fast enough for practical experimental work.

The stop-flow experiments help us determine the role of relaxation, if any, on the present experimental results. The 10 min interval following injection, in which no flow occurs, is more than adequate to achieve relaxation with the present range of experimental parameters. Relaxation under static conditions does not perturb *R* values. Table 1 shows a comparison of stop-flow and continuous-flow results for several experimental

TABLE 1

Comparison of Retention Parameter R measured under Continuous-Flow Conditions (R_{cf}) and Stop-Flow Conditions (R_{sf}). Polystyrene Solutes of the Stated Molecular Weight Are Used in Ethylbenzene Solvent in the 0.254-mm Channel at $T_c = 16°\text{C}$. $\Delta R = R_{cf} - R_{sf}$

MW	ΔT (°C)	R_{cf}	R_{sf}	ΔR
20,000	60	0.69	0.67	0.02
51,000	60	0.47	0.43	0.04
97,000	33	0.53	0.52	0.01
97,000	60	0.33	0.32	0.01
160,000	20	0.64	0.65	−0.01

conditions. The stop-flow results yield R values slightly below (0.014 R units average) the continuous-flow levels. Oddly enough, the polymer of the highest molecular weight, which is retained with the lowest ΔT, showed the opposite effect, even though relaxation effects should theoretically be greatest in this case.

All things considered, we regard relaxation as having only a minor influence on the present results, probably no larger than 0.01 to 0.02 R units.

We present the results of our studies on the variation of different parameters in TFFF below.

Channel Width

Equation (17) has no explicit dependence on channel width, w. Parameter $\beta = B\Delta T/T_c^2$, contained therein, will not vary with w under fixed conditions of temperature, temperature drop, and solvent. Parameter $\lambda = \ell/w$, also contained in Eq. (17), may be written as follows using Eq. (3):

$$\lambda = \frac{1}{\left(\frac{\alpha}{T} + \gamma\right)\frac{dT}{dx}w} \tag{20}$$

If dT/dx is equal to $\Delta T/w$,

$$\lambda = \frac{1}{\left(\frac{\alpha}{T} + \gamma\right)\Delta T} \tag{21}$$

an expression independent of w. Even if dT/dx is assumed proportional—

TABLE 2

The Variation of Retention Parameter R with Channel Width w for Various Polystyrene Molecular Weights in Toluene at $T_c = 20°\text{C}$ and $\Delta T = 32°\text{C}$

MW	R	
	$w = 0.254$ mm	$w = 0.127$ mm
19,800	0.87	0.88
51,000	0.72	0.73
97,000	0.56	0.60
160,000	0.44	0.47

not equal—to $\Delta T/w$, the same conclusion is reached. (Proportionality, only, would be applicable if variation in thermal conductivity was considered.)

Because Eq. (17) and the parameters it contains show no variation of a solute's retention with w under specified thermal and solvent conditions, it is predicted that retention parameter R will remain constant with changes in w at fixed ΔT, T_c, and B. Table 2 provides a test for this conclusion. It shows the results of an experimental study in which channels of widths 0.254 and 0.127 mm are compared. It is seen that, for each solute, the R value measured in the wider channel is slightly lower than its value in the narrow channel. (The opposite result would have occurred if relaxation had any significant role.) However, the difference averages just over 0.02 R units, which is not very significant experimentally. We therefore conclude that the prediction of theory is essentially valid, and that for practical purposes retention parameters do not vary with channel width w.

Molecular Weight

Increases in solute molecular weight (MW) lead to increasing retention (decreasing R) in TFFF, other things being constant. Thus in polymer mixtures, low molecular weight polymers are eluted first (*1*). The general trend of R vs MW curves is shown in Fig. 6 where experimental results are presented for four polystyrenes of different molecular weight at four different ΔT values.

A simple rule governs, to a reasonably good approximation, the molecular-weight dependence of retention. If the γ term of Eq. 20 is dropped by virtue of its small relative magnitude,

$$\lambda = \frac{T}{\alpha w(dT/dx)} \tag{22}$$

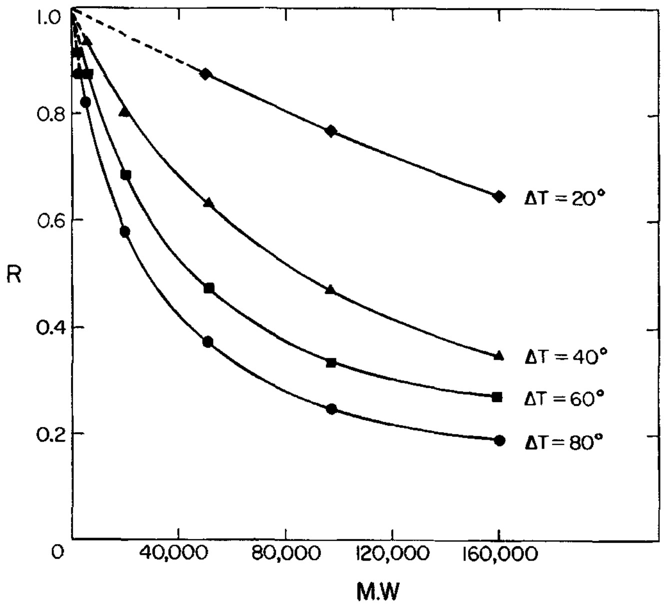

Fig. 6. Retention parameter R vs MW of polystyrene solute in ethylbenzene solvent. $T_c = 16\,^{\circ}\mathrm{C}$.

It was noted just prior to Eq. (2) that α is defined in terms of the thermal diffusion coefficient D' and the ordinary diffusion coefficient D by $\alpha = D'T/D$. The substitution of this into Eq. (22) gives

$$\lambda = \frac{D}{D'w(dT/dx)} \tag{23}$$

Diffusion coefficient D for dilute polymer solutions varies approximately as $1/(\mathrm{MW})^{1/2}$ (*13*). It was noted earlier that D' is essentially independent of molecular weight. When these conclusions regarding D and D' are substituted into Eq. (23), the molecular-weight dependence of λ is predicted to be

$$\lambda = \frac{\text{constant}}{(\mathrm{MW})^{1/2}} \tag{24}$$

This conclusion is tested by converting the experimental R values of Fig. 6 to λ values through Eq. (17), then plotting the λ values so obtained against $1/(\mathrm{MW})^{1/2}$. The results are shown in Fig. 7. It is seen that the forecast

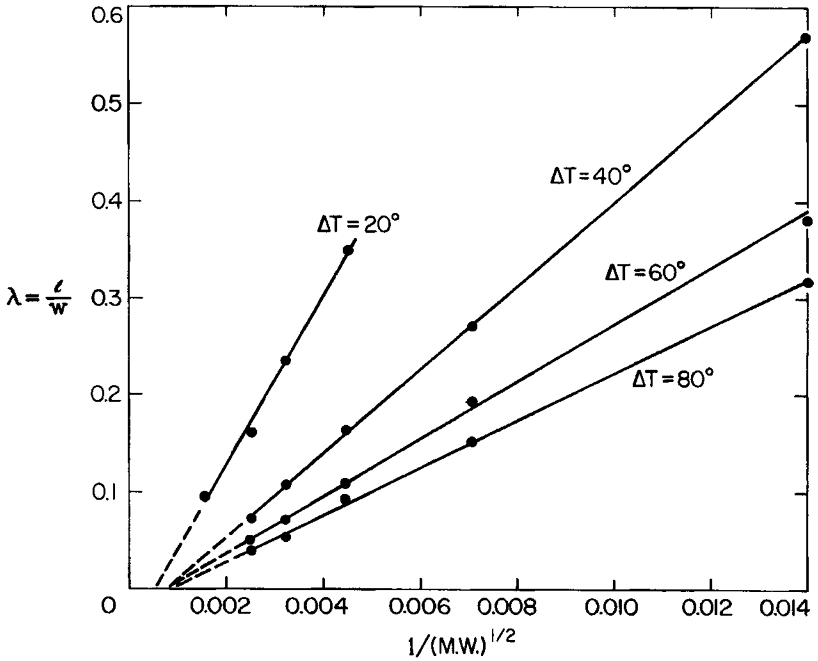

Fig. 7. Plots of λ vs $1/(\mathrm{MW})^{1/2}$ for several ΔT's at $T_c = 16\,°\mathrm{C}$, showing an approximate straight-line dependence.

provided by Eq. (24) is generally successful in describing the trend of molecular-weight effects. It is interesting, however, that the slopes do not pass exactly through the origin as predicted, but intercept the $1/(\mathrm{MW})^{1/2}$ axis at a value corresponding roughly to a molecular weight of 2 million.

Channel Temperature Drop

The temperature drop across the channel, ΔT, is the fundamental cause of the thermal diffusion that underlies retention. One naturally expects, therefore, to see retention increase (R decrease) with increasing ΔT. This expectation is verified for ethylbenzene carrying polystyrene solutes in six different molecular-weight categories by Fig. 8. The R curve for each particular solute starts at unity, then plummets with increasing ΔT. The effect is most pronounced for components of higher molecular weight, as expected.

The precise nature of the R vs ΔT curves relates to the way that λ

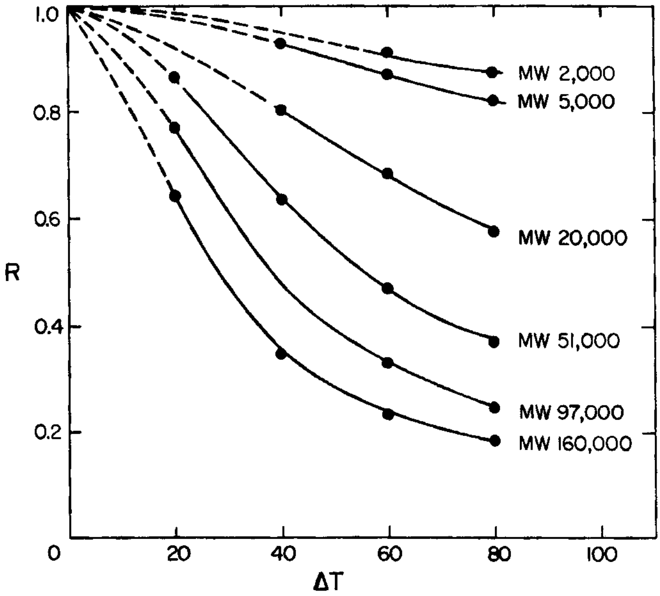

FIG. 8. Retention parameter R vs ΔT for polystyrene solutes of different molecular weights at 16 °C.

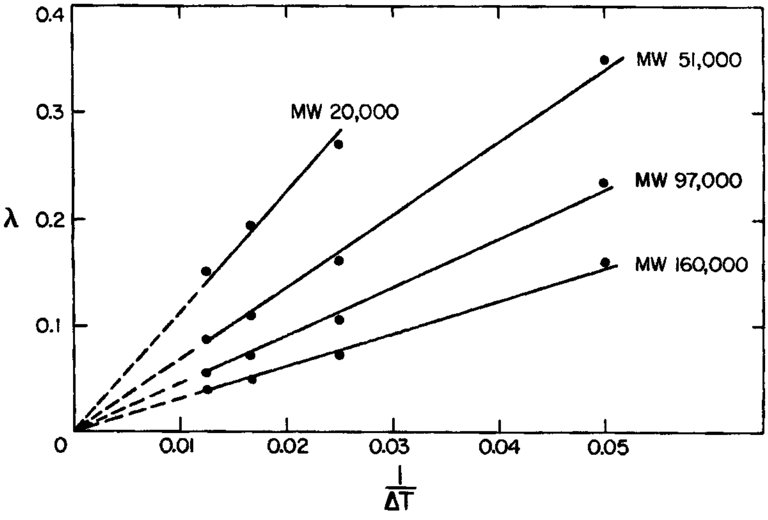

FIG. 9. Plots of λ vs $1/\Delta T$ for polystyrene solutes of different molecular weights in ethylbenzene. The cold-wall temperature is 16 °C.

depends on ΔT. This is shown explicitly in Eq. (21). While this expression is not rigorously correct if the gradients in thermal conductivity are considered, it should be accurate enough to provide a simple guide to retention variations in TFFF. Figure 9 verifies the predicted trend. Here λ is plotted against $1/\Delta T$ for four different polystyrene solutes. The results are in good accord with the expectation that straight lines will be formed which intercept the origin.

Cold-Wall Temperature

Figure 10 shows the dependence of R on cold-wall temperature, T_c, at a fixed temperature drop, $\Delta T = 40\,^\circ\mathrm{C}$. The values of R are seen to increase with T_c, but not to any significant extent. For the slight variations in T_c anticipated in laboratory practice, R may be considered as virtually constant. However, it is interesting to speculate on the origin of the effect, despite the lack of great practical significance.

The slight changes in R with T_c reflect small changes in λ, and ultimately in the basic thermal diffusion parameters, α and D'. No clear temperature

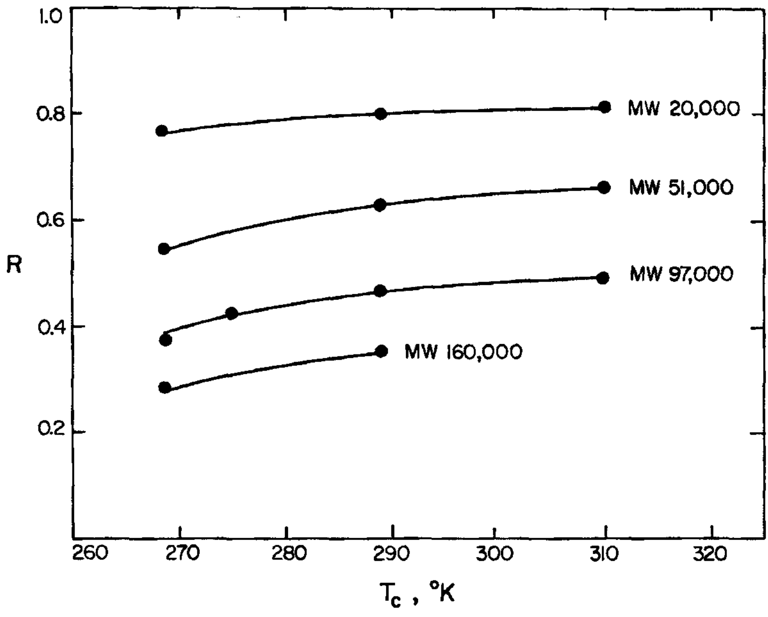

FIG. 10. The variation of R with cold-wall temperature for various polystyrene solutes in ethylbenzene at $\Delta T = 40\,^\circ\mathrm{C}$.

dependence has been established in the literature for the thermal diffusion coefficient, D'. If the temperature dependence of D' is negligible, λ (and R) will follow the temperature dependence of diffusion coefficient D, as shown by Eq. (23). This would explain the slight upward trend of Fig. 10. However, the uncertainties in literature studies on D' make it impossible to claim a sound theoretical footing for the results observed here. At present, the best evidence from any source on the temperature dependence of D' for polymers comes from Fig. 10 itself. These results, of only secondary importance here, will be reported later (*7*).

Sample Size

Increasing quantities of polymer in the solute sample will cause complicated intermolecular interactions, having, ultimately, an effect on both D' and D. Since this effect will be concentration dependent, and thus greatest at the cold wall, the concentration distribution will be perturbed from its normal exponential form shown by Eq. (4). Distortion of the axial zone profile is also expected as a consequence of these nonlinearities. There is not sufficient theoretical or experimental evidence at hand to predict the outcome of sample-size variations. This is, at present, strictly an empirical matter, and will be so treated below.

Figure 11 shows two separate plots of R vs milligrams of polymer sample. The top plot stems from work in which different volumes of a standard solute–solvent mixture (25 mg/ml) were injected. The bottom plot reports the effects of different amounts of solute in a fixed volume of the ethylbenzene solvent (10 μl). These plots are intended to distinguish between the effects of sheer sample volume and of concentration, if any.

In both cases, R decreases gradually with sample size. When the sample size reaches a level just under 1 mg, significant peak tailing appears. This develops rapidly into a second peak, trailing slightly behind the first. The R values of both the trailing and primary peaks are shown in the figure as two separate branches.

The overall trends of the two plots of Fig. 11 are very similar, showing no significant influence of the volume in which the stated weight of polymer is dissolved. The only noticeable divergence is in the trailing peak, which seems to become even more retarded when the sample is introduced in concentrated form.

The usual sample size employed in the work of this paper was 0.2 mg. This provides a mixture near enough to infinite dilution that no significant changes are expected to take place with further dilution. Figure 11 shows

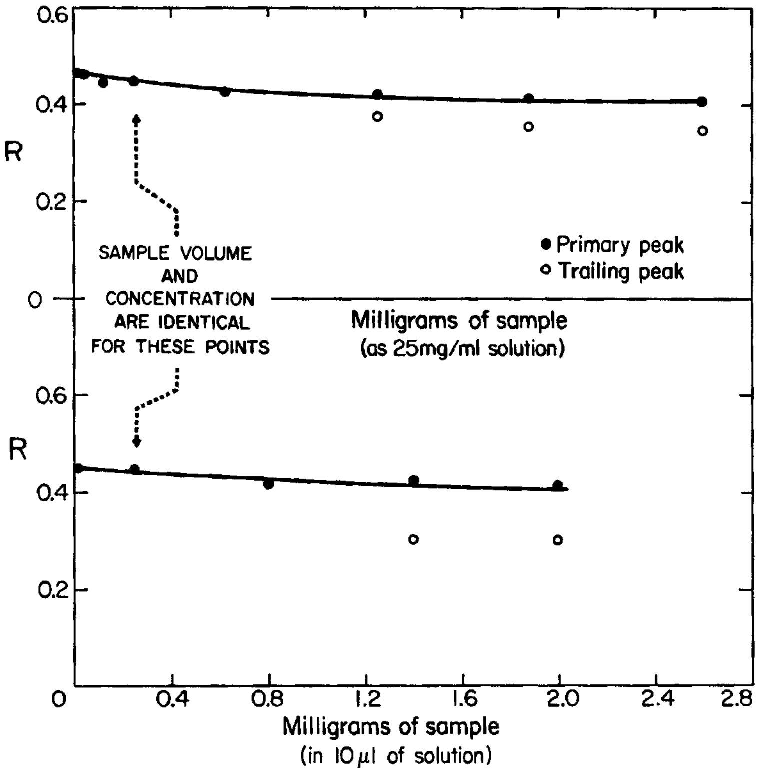

FIG. 11. Dependence of *R* on sample size in milligrams of 97,200 MW polystyrene at $\Delta T = 40$ °C and $T_c = 16$ °C. Top curve is for constant sample concentration and bottom curve is for constant sample size (see text).

that *R* values would not increase more than about 0.01 units as infinite dilution is approached.

Solvent Effects

We have noted that a theoretical basis does not exist for predicting the magnitude of thermal diffusion effects in liquids. In addition, experimental data are scarce. Very few solvents, especially, have been investigated with respect to the degree of thermal diffusion generated with dissolved macromolecules. In this light, we undertook an empirical study of retention in TFFF using a variety of solvents. Most of these were typical organic solvents, but a number contained water or other polar substances. The

TABLE 3

Retention Parameters for Four Polystyrene Polymers in Eight Different Organic Solvents

			MW 19,800		MW 51,000		MW 97,000		MW 160,000	
Solvent	B (°K)	ΔT (°K)	R	λ	R	λ	R	λ	R	λ
Chloroform	885	22	1.00	—	0.93	0.50	0.85	0.33	0.79	0.27
Methyl ethyl ketone	915	32	0.86	0.34	0.73	0.20	0.61	0.15	0.46	0.11
Ethyl acetate	985	33	0.90	0.41	0.75	0.22	0.61	0.15	0.55	0.13
Dimethylformamide	1145	30	0.93	0.50	0.84	0.32	0.72	0.22	0.61	0.16
Dioxane	1545	31	0.89	0.41	0.75	0.20	0.61	0.15	0.51	0.13
Toluene	1085	19	0.94	0.53	0.88	0.36	0.78	0.24	0.69	0.18
		32	0.88	0.37	0.73	0.21	0.60	0.14	0.47	0.10
Ethylbenzene	1095	20	—	—	0.88	0.36	0.77	0.21	0.64	0.16
Cyclohexane	1525	20	0.93	0.57	0.87	0.36	0.77	0.23		
		31			0.69	0.20	0.66	0.18		

information obtained yields important preliminary guidelines on solute–solvent systems suitable for TFFF work.

Table 3 summarizes the experimental results for polystyrene polymers in ordinary organic solvents. These results were obtained in the narrow channel, $w = 0.127$ mm, with the cold wall at 17 °C. In general (except where duplicate or triplicate runs appear) the maximum possible ΔT was used, consistent with the capacity of the cooling system then employed to maintain the stated cold-wall temperature. Because of variable thermal conductivities, ΔT values differ from solvent to solvent.

The results of Table 2 were all normalized to a ΔT of 25 °C by using the relationship $\lambda = \text{constant}/\Delta T$, Eq. (21). The λ corresponding to this ΔT value, termed $\lambda_{25}°$, was then plotted against $1/(\text{MW})^{1/2}$, Fig. 12. Although some of the data exhibit moderate curvature, a group of least-square, straight-line plots through the origin were constructed. These are shown in the figure. Plotted in this way, the slopes of the straight lines are invesely proportional to D' for polystyrene in the respective solvents (Eqs. 23 and 24). Thus the lowest straight-line plot in Fig. 12, for ethylbenzene, corresponds to the largest thermal diffusive interaction and thus the largest D'.

The remarkable thing about these plots is that the best solvents for thermal diffusion are clustered together despite their considerable chemical diversity, as if some ceiling existed to the magnitude of the effect obtainable. Six of the eight solvents exhibit slopes within 20% of one another. Thermal diffusion effects for the other two solvents are weakened only by about 50% relative to the best solvents. These results would suggest that thermal diffusion of a rather constant magnitude is to be expected for most variations in solvent. However, results of the next few paragraphs show that this conclusion is not applicable to aqueous solutions.

In one study of aqueous mixtures, the retention of Blue Dextran (Pharmacia Fine Chemicals, Inc.), with a nominal molecular weight of 2×10^6, was examined in water–DMSO mixtures over a wide concentration range. No retention was observed in pure water nor in DMSO solutions up to 50 vol% DMSO. With further increases in the concentration of DMSO, retention grew rapidly to substantial levels. This is documented in Fig. 13.

Similar results were recorded with other aqueous systems. The proteins albumin (bovine serum) and hemoglobin (bovine), as well as Blue Dextran, were injected into various aqueous buffers and into water mixed with 2 and 6 M guanidine hydrochloride and with 8 M urea. In none of these cases was significant retention detected.

In summary, TFFF does not appear to cause effective retention in most

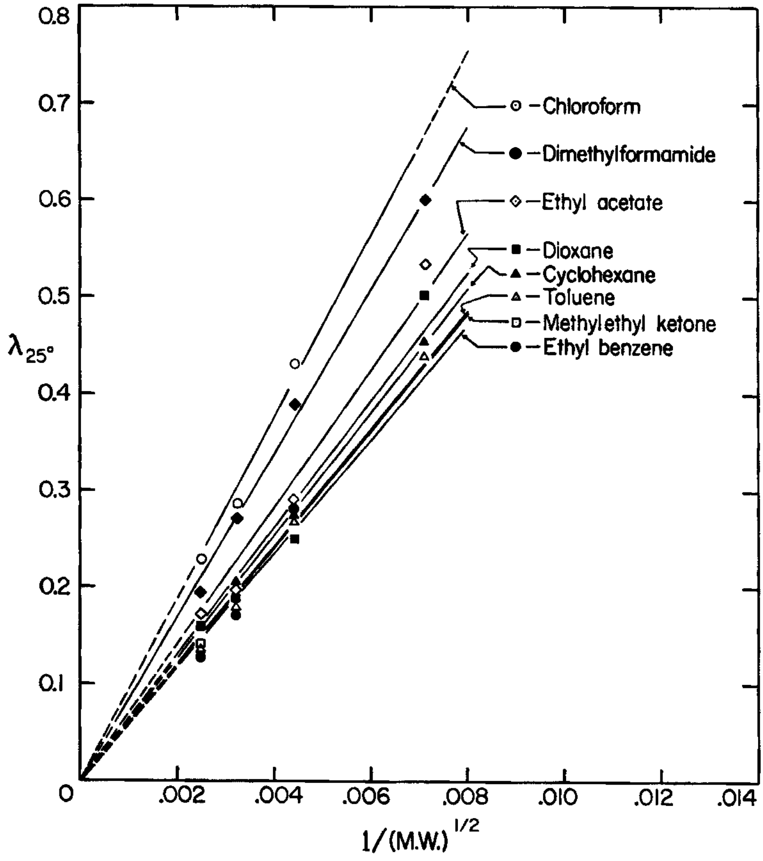

FIG. 12. The effect of solvent on retention parameter λ for different molecular weights. Effective $\Delta T = 25\,°C$.

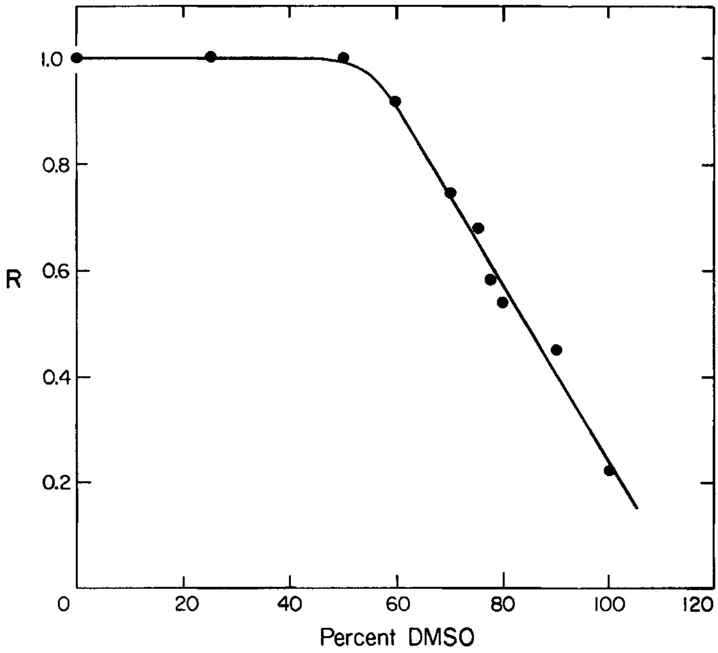

FIG. 13. Retention parameter R vs volume percentage of DMSO in aqueous solution using Blue Dextran solute. Results were normalized to $\Delta T = 45\,^\circ\mathrm{C}$.

aqueous solutions, but it shows significant levels of retention for polystyrene polymers in various organic solvents. The degree of retention responds rationally to various parameter changes, making the control of retention a relatively simple task. This controllability is an advantageous feature of TFFF as a tool in macromolecular separations.

Acknowledgments

This investigation was supported by Public Health Service Research Grant GM 10851–16 from the National Institutes of Health. Mr. Lyle Bowman is gratefully aknowledged for making the computer runs leading to Fig. 5.

REFERENCES

1. G. H. Thompson, M. N. Myers, and J. C. Giddings, *Anal. Chem.*, *41*, 1219 (1969).
2. M. E. Hovingh, G. H. Thompson, and J. C. Giddings, *Ibid.*, *42*, 195 (1970).
3. K. E. Grew, in *Transport Phenomena in Fluids* (H.J.M. Hanley, ed.), Dekker New York, 1969, Chap. 10.

4. J. C. Giddings, M. E. Hovingh, and G. H. Thompson, *J. Phys. Chem.*, *74*, 4291 (1970).
5. P. H. Norberg and S. Claesson, *Acta Imeko*, *4*, 501 (1964).
6. G. Meyerhoff, H. Lütje, and B. Ranch, *Makromol. Chem.*, *44–46*, 489 (1961).
7. K. D. Caldwell, M. N. Myers, and J. C. Giddings. To Be Published.
8. H. J. V. Tyrrell, *Diffusion and Heat Flow in Liquids*, Butterworths, London, 1961.
9. J. C. Giddings, *J. Chem. Phys.*, *49*, 1 (1968).
10. J. C. Giddings, *J. Chem. Educ.*, *50*, 127 (1973).
11. J. Hoppel and H. Brenner, *Low Reynold's Number Hydrodynamics*, Prentice-Hall, Englewood Cliffs, New Jersey, 1965, p. 34.
12. J. C. Giddings, *Separ. Sci.*, *8*, 567 (1973).
13. P. J. Flory, *Principles of Polymer Chemistry*, Cornell Univ. Press, Ithaca, New York, 1953.

Received by editor August 12, 1973